ZERO – CURRENT SWITCHING OF RESONANT INVERTER FOR CONTACTLESS INDUCTIVE POWERING TRANSMISSION SYSTEMS OVER LONG AIR–SEPARATION [+]

تحويلات التيار–الصفري للعاكس الرنيني المستخدم في منظومات القدرة الكهربائية الحثية اللاتلامسية

Abd- ALjabar .F. ALI [*]

ABSTRACT

The proposed high frequency inverter circuit is devoted to analyze the behavior of contactless inductive powering transmission system with large air separation. Typical applications are for automatic battery charging station and for power supply of inductively powered electric vehicles and other movable consumers. The paper investigates the influence of geometrical and electrical parameters on power transmission with air-separation of (1000mm) through zero-switching state simulation of the proposed high frequency inverter. Contactless powering transmission systems operate at resonance frequency with a proper choice of the resonance capacitor on the primary and secondary side, the contactless system represents an ohmic load for the primary inverter. Therefore switching events take place at zero current (ZCS) without auxiliary commutation elements, which is an important precondition for reaching higher transmission frequencies. For this application a special inverter was developed. The phase–shifted controlled bridge at the primary side is equipped with Insulated-Gate bipolar transistors and freewheeling silicon carbide schottky diodes. Because of their ultra low reverse recovery charge, the operation behavior is much better as compared with fast silicon diodes.

المستخلص :

في السنوات الأخيرة – تطورت تقنية نقل الطاقة الكهربائية اللاتلامسية وخصوصا في تطبيقات الشحن الـذاتي لبطاريات المحطات وكذلك في تطبيقات العربات الكهربائية وتطبيقات حديثة أخرى. يتناول البحـث تـأثير المتغيـرات الهندسية والكهربائية على نقل هذا النوع من الطاقة بفجوة هوائية(١٠٠٠ملم) وذلك من خـلال تحـويلات التيـار–الصفري للعاكس الرنيني المقترح في هذا البحث. يتحقق نقل الطاقة اللاتلامسية بـالتردد الرنينـي لهـذا العـاكس، فبالاختيار الأمثل للتردد الرنيني السعوي على كل الطرفين الابتدائي والثانوي للمحولة اللاتلامسية يتماثل المنظومـة إلى الحمل ألمقاومي مما يؤدي إلى حصول حالات التحويل عند التيار–الصفري وبـدون اسـتخدام عناصـر إخمـاد مساعدة لهذا العاكس. إن هذه الطريقة تعتبر من أهم الحالات المسبقة للوصول إلى توليـد التـرددات العاليـة لهـذا العاكس الرنيني المقترح باستخدام (IGBTS) مع دوائر ثنائي الإطلاق بنوعين مختلفين.

KEYWORDS
>> flux model <<, >> magnetic devices <<, >> contactless power transmission <<, >> high frequency inverter <<, >> schottkey diodes <<.

[+] **Received on 23/7/2009 ,Accepted on 26/10/2010 .**

[*] **Ass . Prof / Technical Institute/Umara**

INTRODUCTION

For an increasing number of applications in mechanical engineering, production technology, transportation and medical engineering there are promising application prospects for contactless inductive powering transmission system. Typical applications are robots machines tools, linear movable systems and non-contact battery chargers for electric vehicles [1-4]. By means of the contactless transmission technology trailing cables can be replaced and therefore cable breaks can be a voided other advantages are: no wear and tear on the electric contacts [5-7]. No contact resistance, no sparking (can be used in explosion endangered environment) and no non-protected voltage carrying contacts. The extension of the contactless power transmission to longer distances opens new application fields for this electricity supply technology.

MAGNETIC ASSEMBLIES CIRCUITS :

1- EQUIVALENT CIRCUIT

Figure 1 shows the equivalent electric circuit of the magnetic assemblies with large air-separation (E-E, E-I, I-I) type. The figure contains the magnetizing inductance (L_h) the leakage inductances $L_{1\sigma}$, $L_{2\sigma}$ and the ohmic resistances of the winding (R_1, R_2). The magnetizing inductance and the leakage inductances of the contactless systems mainly depend on the dimension of the primary and secondary system, the existence of ferrite cores on the primary or secondary side and the air-separation length. Contactless transmission systems are characterized by a very small magnetizing inductance and large leakage inductances. Especially for power transmission over a large air-separation a careful geometrical optimization is necessary by means of magnetic flux simulation as showing in Fig.2. The simulation techniques are carried out with the help of ANSYS and MATLAB programs.

Fig.3 shows the magnetic flux lines of an optimized magnetic assembly with (L=1000 mm) air-separation. The primary and secondary coils have a diameter of (D=400 mm) pancake-shape coils. The inductances (L_h, $L_{1\sigma}$, $L_{2\sigma}$) can be obtained by magnetic flux simulation. Starting from the magnetic flux distribution of the applied geometry [8].

$$L_h = N_1^2 \frac{\Phi_{2NL}}{i_{1NL}} \qquad \text{.....(1)}$$

$$L_{1\sigma} = N_1^2 \frac{\Phi_{1NL} - \Phi_{2NL}}{i_{1NL}} \qquad \text{.....(2)}$$

$$L_{2\sigma} = N_2^2 \frac{\Phi_{1L} - \Phi_{2L} - L_{1\sigma} i_{1L}}{i_{2L}} \qquad \text{.....(3)}$$

At first only the primary coil is fed by the current i_{1nL}. As a result of the magnetic flux simulation the primary and secondary fluxes can be obtained.

OUTPUT POWER TRANSMISSION CHARACTERISTICS:

A fundamental problem of contactless powering transmission system is the large secondary leakage inductances. Consequently, the transfer of appreciable electric power requires the compensation of the leakage inductances. The series resonance capacitors on the primary and secondary sides can be determined by means of equation (4) and (5) [8].

$$C_1 = \frac{1}{N_1^2\left(L_{1\sigma 0} + \frac{L_{h0} + L_{2\sigma 0}}{L_{h0} + L_{2\sigma 0}} \right)\omega_{res}^2} \qquad \text{---------- (4)}$$

$$C_2 = \frac{1}{N_2^2 \left(L_{h0} + L_{2\sigma 0}\right)\omega_{res}^2} \qquad \text{---------- (5)}$$

At the resonance operating point of the contactless transmission system, the output power is contained in equation (6) and the efficiency in equation (7) as a function of the secondary load resistance. The output power mainly depends on the magnetizing inductance, the square of the primary magneto-motive force $(N_1 * i_1)^2$ and on the transmission frequency [8].

$$P_2 = \left(N_1 i_1\right)^2 \left[\frac{L_{h0}}{N_2\left(L_{h0} + L_{2\sigma 0}\right) + \frac{R_{20} R_L}{N_2\left(L_{h0} + L_{2\sigma 0}\right)\omega_{res}^2}} \right]^2 * R_L \qquad \text{---------- (6)}$$

$$\xi = \frac{R_L}{R_L + \frac{R_{10}\left[N_2^2\left(L_{h0} + L_{2\sigma 0}\right)^2 \omega_{res}^2 + R_{20} R_L\right]^2}{N_2^2 L_{h0}^2 \left(L_{h0} + L_{2\sigma 0}\right)^2 \omega_{res}^2} + N_2^2 R_{20}\left[1 + \left(\frac{R_L}{N_2^2\left(L_{h0} + L_{2\sigma 0}\right)\omega_{res}} \right)^2 \right]} \qquad \text{----- (7)}$$

Fig.4 shows the output power (equation 6) and the efficiency (equation 7) of a contactless power transmission system as a function of the secondary load resistance. A transmission frequency of (50 kHz) is used. The output power as well as the efficiency have a maximum at different load resistances (26.45 kW) and (85.4 %) respectively.

Fig.5 shows the output power at maximum efficiency operating point for different transmission frequencies as a function of air–separation lengths, whereby the output power is related to the square of the primary magneto-motive force. The reachable output power strongly decreases with the air–separation length nearly in the same way as the magnetizing inductance, on the other hand by using higher transmission frequencies greater than (100 KHZ). The transferable electric output power and the efficiency of the contactless systems can be increased considerably. Moreover, high transmission frequencies lead to smaller filter elements and ferrite components. This effect is limited by the increase of the ohmic resistance of the windings due to skin and proximity effect and the increase of ferrite losses at about (150 KHZ).

1- ELECTIC CIRCUIT TOPOLOGY

For contactless power transmission at high frequencies, the special inverter in Fig.6 was proposed. The phase–shifted controlled IGBT bridge at the primary side converts the constant rectified line voltage into an AC voltage with variable amplitude and frequency up to

150 KHZ. The inverter bridge has to be switched according to the pulse pattern in Fig.7. Each IGBT is switched on over half a period. The phase shift of the firing signals for the semiconductors S_1/S_2 and S_3/S_4 is in the range of (Φ = 0 - 180°). The IGBT S_2 requires the inverted signal of S_1 and the IGBT S_4 needs the inverted signal of S_3. Between the original and the inverted firing signals, the delay time (t_v) is necessary in order to a void short circuit currents.

With a proper choice of the resonance capacitors the contactless system represents an ohmic load for the primary inverter. Fig.8 shows the inverter output voltage and current at rated load of the contactless transmission system at a transmission frequency of (100 kHz). The primary current is nearly sinusoidal without any harmonics, because the contactless resonance transformer acts as a second order filter. The phase angle between the primary voltage and current is nearly zero. Therefore, at maximum pulse width of the inverter, the switching events can take place at zero current without auxiliary commutation elements. This zero current switching (ZCS) is an important precondition for reaching higher transmission frequencies. However if the output voltage and current of the primary inverter are in–phase, non –permitted switching actions occur which can destroy the IGBTS. Such dangerous switching actions take place if an IGBT is turned on when the opposite anti-parallel freewheeling diode of the same bridge leg conducts the current. As an example, the commutation from D_4 to S_3, which is initiated by switching on S_3 is cleared from the figure. In this case the diode D_3 does not get enough reverse recovery times to restore its blocking capability. This inadmissible operation state leads to short circuits in the bridge leg, increased losses and destruction of the IGBTS due to over current. These effects, which result from the non-permitted commutation is increased at reduced pulse width of the inverter (low load operation of the contactless system. In this case the current through the freewheeling diode D_4 is relatively high when the opposite IGBT is turned on.

Therefore contactless transmission systems can not be operated in (ZCS) mode if the primary inverter is equipped with fast s_i freewheeling diodes. For a safe operation of the inverter from rated load to low load, the contactless system has to be adjusted inductively. Therefore the advantages of (ZCS) can not be used and higher switching frequencies can not be realized in the power range of several kilo watts.

2- FREEWHEELING SIC SCHOTTKY DIODES

The main benefit of s_{ic} schottky diodes which will be exploited in this special application is their very small reverse recovery charge. Moreover, this charge is nearly independent from temperature forward current and (d_i/d_t). The comparison between S_i and S_{ic} diodes is shown exemplary for switching on IGBT S_3 (current commutation from D_4 and D_3) and switching off diode D_3 (current commutation from D_3 and D_4). The comparison is shown in the following figures for the inverter operating point in figures 9 and 10 (low load operation of the contactless transmission system). The results are similar to the rated load operation.

With S_i diodes (figures 9 and 11) the current peak is about 20 A and exceeds the diagram limit for more than l00 nsec. The switching losses are very high (Fig.12). By using sic shottky diodes the current peak is much smaller and the switching losses are lower (Fig.13). However, the amplitude of the voltage oscillation is higher with sic diodes. This results from the parasitic inductances between the DC link capacitor and the power semiconductor devices.

CONCLUSION :

By using higher transmission frequencies greater than 100 kHz, the transferable electric power and the efficiency of contactless power transmission systems can be increased considerably. Moreover, high transmission frequencies lead to smaller filter elements and ferrite components. At the resonance operation, the contactless system represents an ohmic load for the primary inverter. The primary current is nearly sinusoidal and the phase angle between primary voltage and current is zero. Therefore, at the maximum pulse width of the inverter, the switching events could take place at zero current without auxiliary commutation elements. This zero current switching (ZCS) is an important precondition for reaching higher transmission frequencies. However, at this operation point, non-permitted current commutation take place if an IGBT is turned on when the opposite anti-parallel freewheeling diode of the same bridge leg conducts the current. These inadmissible operation states can be avoided using s_{ic} schottky diodes instead of the commonly used s_i freewheeling diodes. Therefore, by using freewheeling sic schottky diodes for this application, the inverter can safely operate in the complete load range.

REFERENCES:

1- Klontz, K.W.; Divan, D.M.; Novotony, D.W.; Lorenz, R.D.:"*Contactless power delivery system for mining applications*". IEEE Transaction on Industry Applications, Vol. 31, No. 1 January / February 1995, pp 27-35.

2- Knaup, P.;Hasse, K.:"*Zero – voltage switching converter for magnetic transfer of energy to movable system*" European Conference On Power Electronics and Applications, Trondheim 1997, Vol. 2, pp 168-173.

3- Hui, S.Y.R., Ho, W.W.C.:"*New Generation of Universal Contactless Battery Charging Platform For Portable Consumer Electronic Equipment*". Power Electronics, IEEE Transactions, Volume: 20 Issue: 3, may 2005, pp 620-627.

4- Hu, A.P., Boys, J.T.;Covic, G.A.; "*Frequency Analysis and Computation of a current – Fed resonant Converter For ICPT power supplies*. International Conference on Vol. 1,4-7 Dec. 2000, pp 327-332.

5- Boys, J.T.; Covic, G.A.; Green, A.W.; "*Stability and Control of Inductively Coupled Power Transfer system" Electric Power Applications*, IEEE Proceeding. Vol. 147, Issue 1, Jan 2000, pp 37-43.

6- Green, A.W.; Boys, J.T.: "*10 kHZ inductively Coupled Power Transmission–Concept and Control".* International Conference On Power Electronics and Variable Speed Drives, London 1994, pp 694-699.

7- Eber, A.; Nagel, A." *Contactless High Speed Signal Transmission Integrated In a Compact Rotatable Power Transmission*". European Conference on Power Electronics, Brighton 1993, Vol. 4, pp 409-414.

8- Ali AJF. " *Finite Element Modeling and Analysis of Contactless Inductive Power Transmission Systems*", PhD Thesis, Basrah University, October 2008.

List of Symbols

Symbol	*Definition*	*Units*
L	*Air-Separation Length*	*mm*
$L_{1\sigma}$	*Primary-Leakage Inductance*	*H*
$L_{2\sigma}$	*Secondary-Leakage Inductance*	*H*
Lh	*Magnetizing Inductance*	*H*
L_{10}	*Self Inductance of the primary Coil*	*H*
L_{20}	*Self Inductance of the secondary Coil*	*H*
N	*Number of terns*	
P_2	*Output power*	*W*
Φ	*Magnetic Flux*	*Wb*
ω	*Angular Frequency*	*Rad.\sec*
D	*Coil Diameter*	*mm*

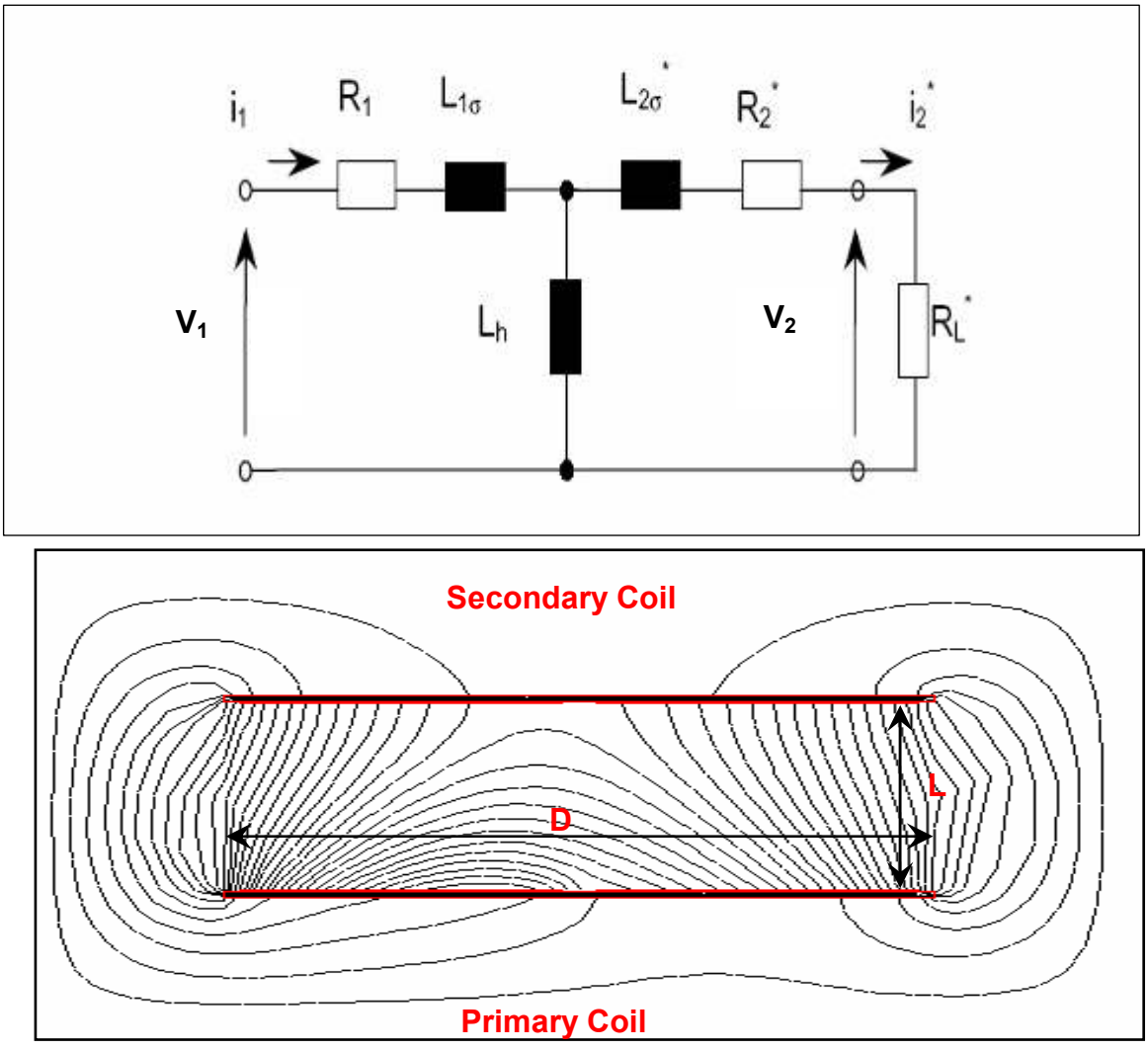

Fig.2: The simplified magnetic assembly with D=800 mm, L=1000 mm

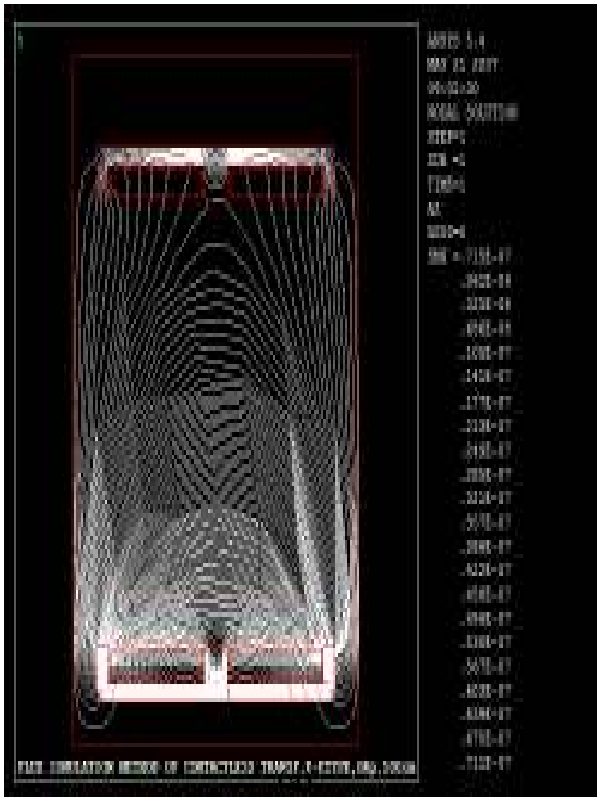

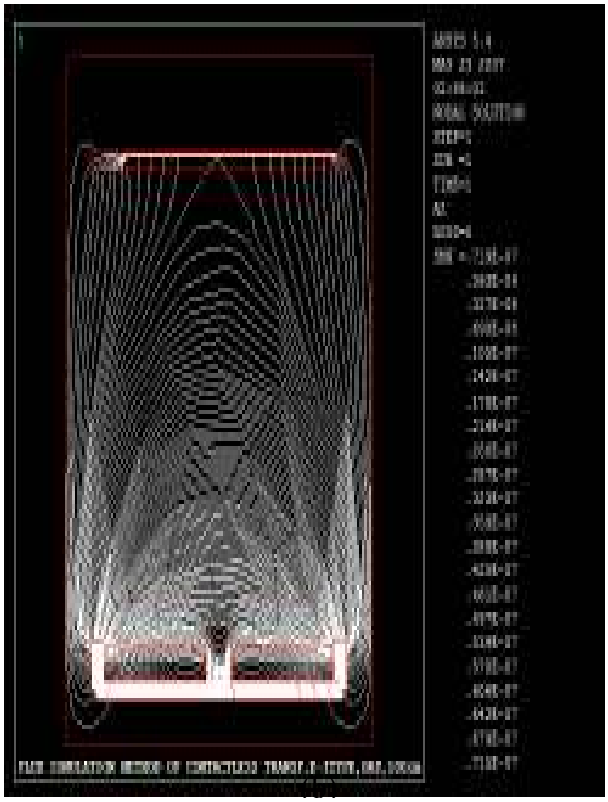

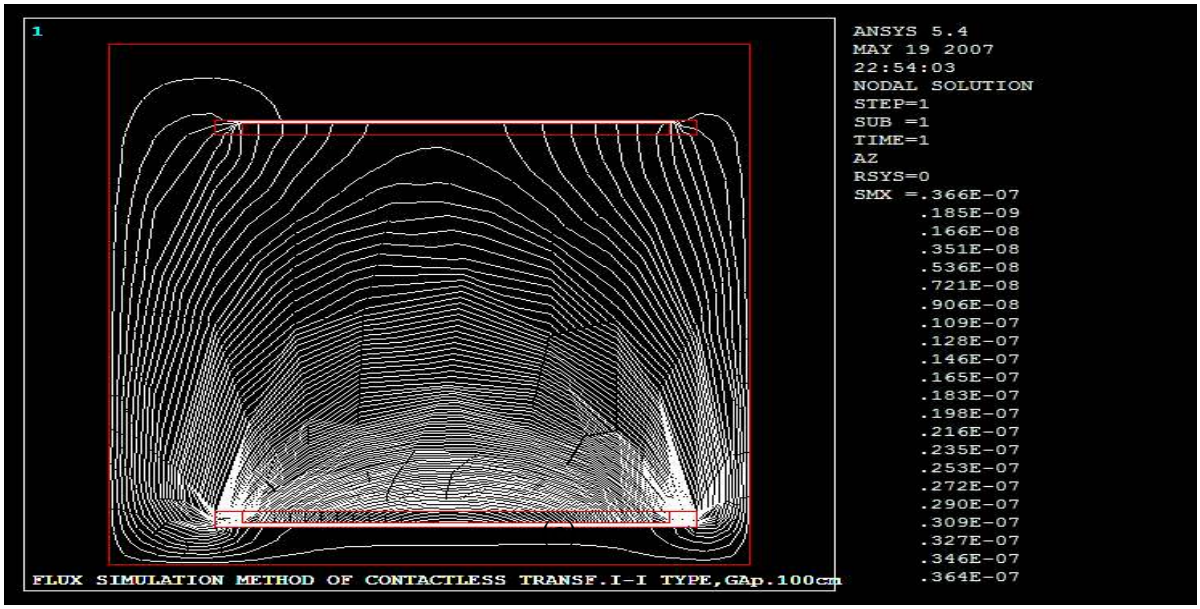

Fig.3: Magnetic flux lines of a contactless power transmission assemblies.
(a) E-E type (b) E-I type (c) I-I type

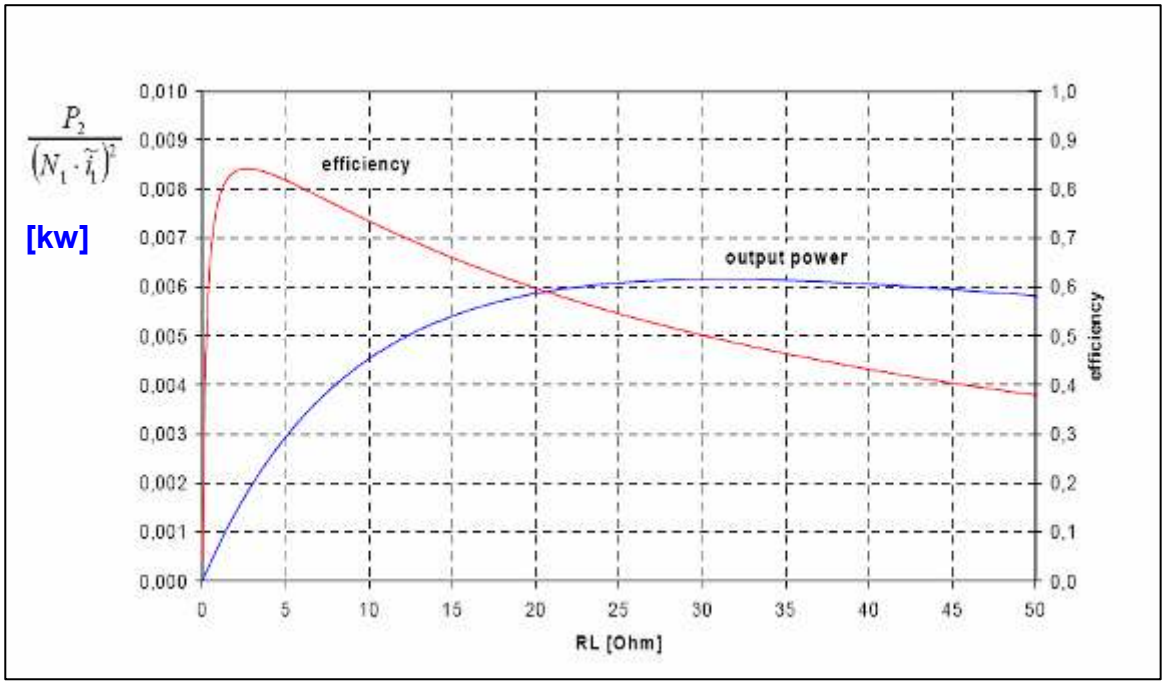

Fig.4: Output power and efficiency as a function of secondary load resistance

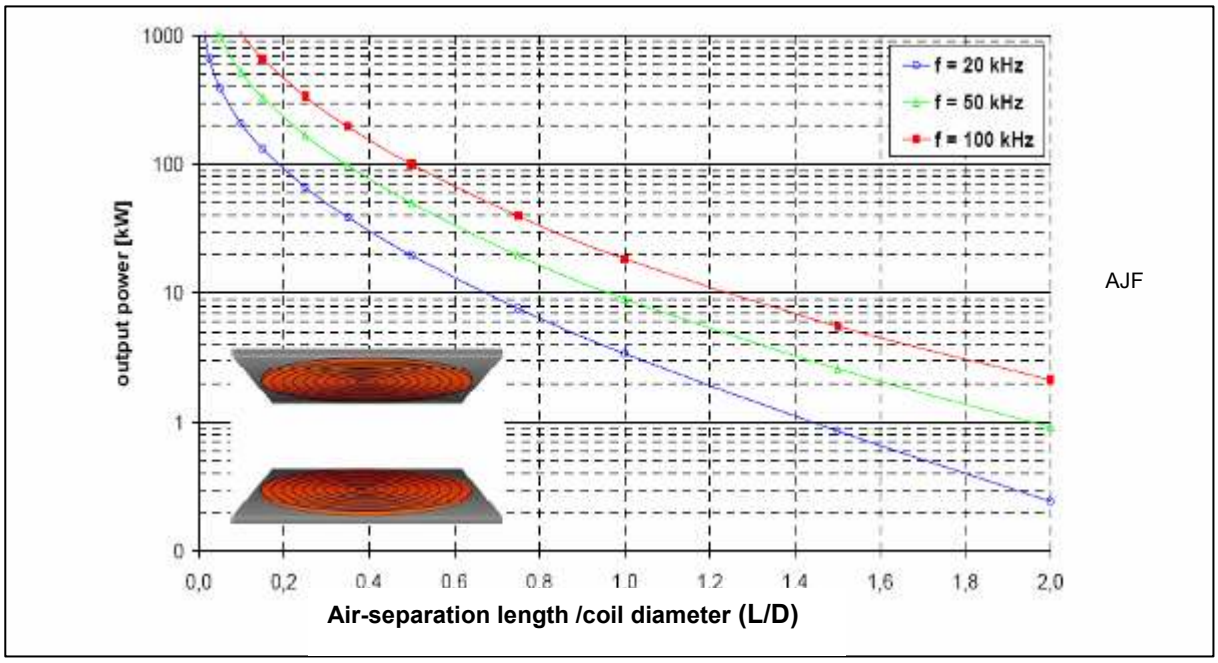

AJF

Fig. 5: Output power for different transmission frequencies as a function of air- separation length

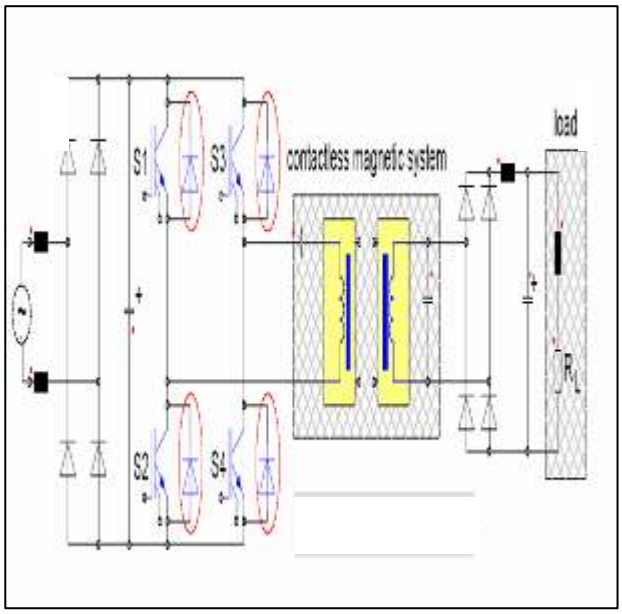

Fig.6: High frequency inerter with freewheeling Sic schottky diodes

00

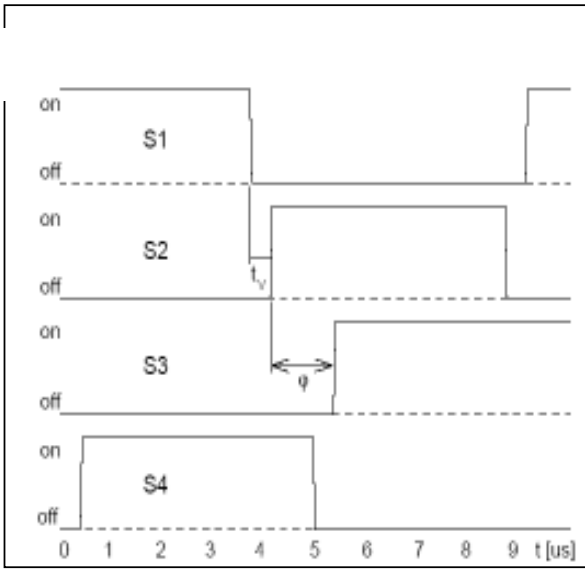

Fig.7:Pulse pattern for phase – shifting modulation

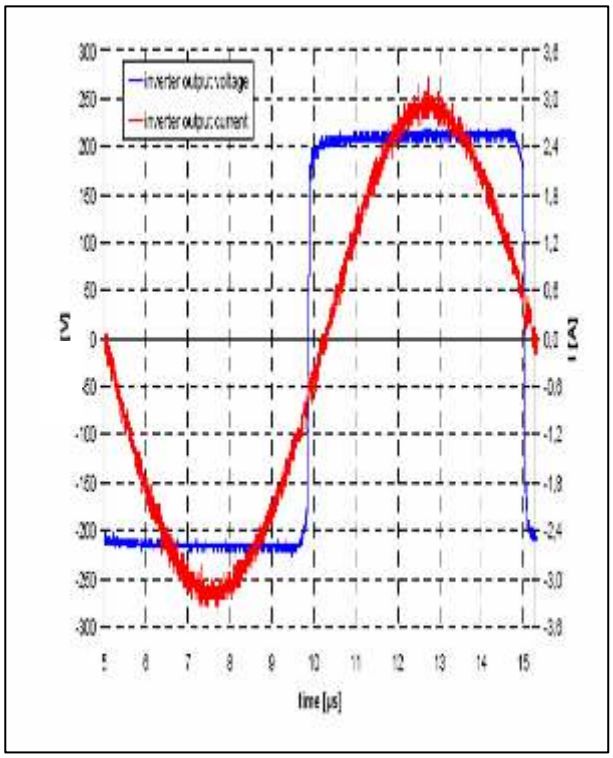

Fig.8: Inverter output voltage and current at rated load of the contactless system system.

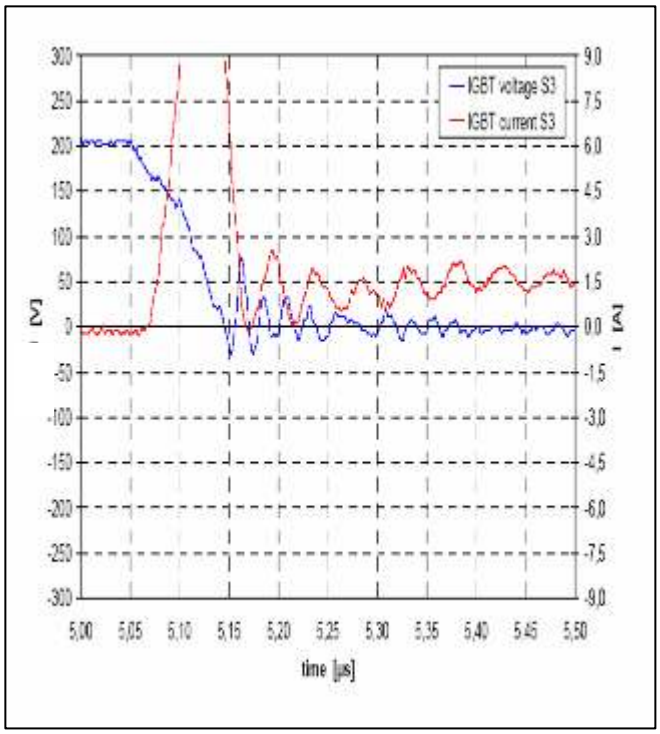

Fig.9: Switching on S3 with fast Si diode

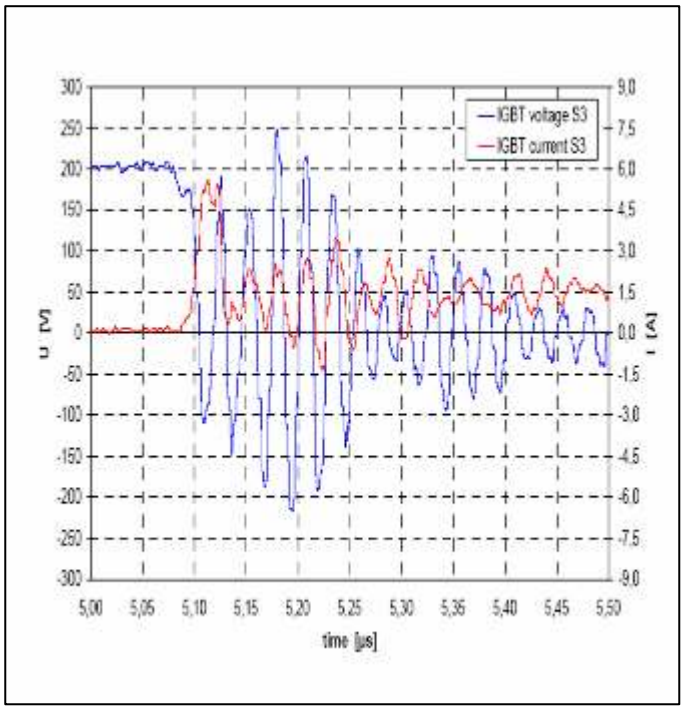

Fig.10: Switching on S3 with Sic Schottky diode

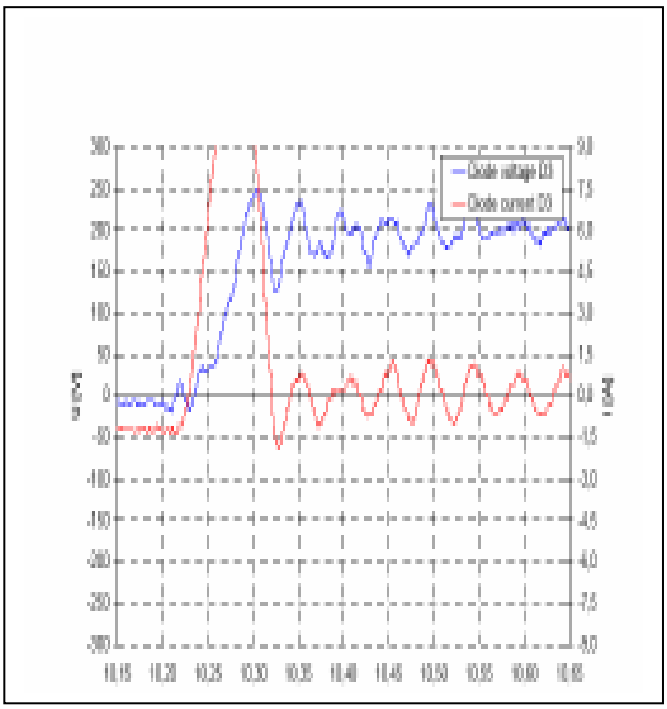

Fig.11: Switching off D3 with fast Si diode

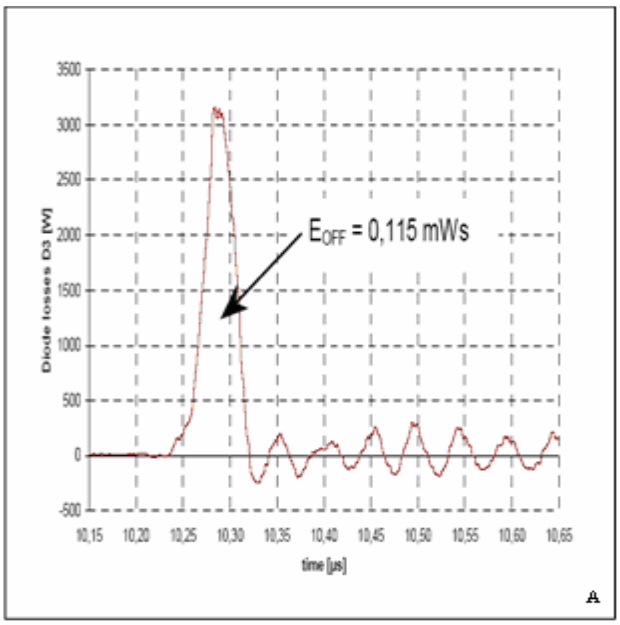

Fig.12 : Switching off D3 with fast Si diode

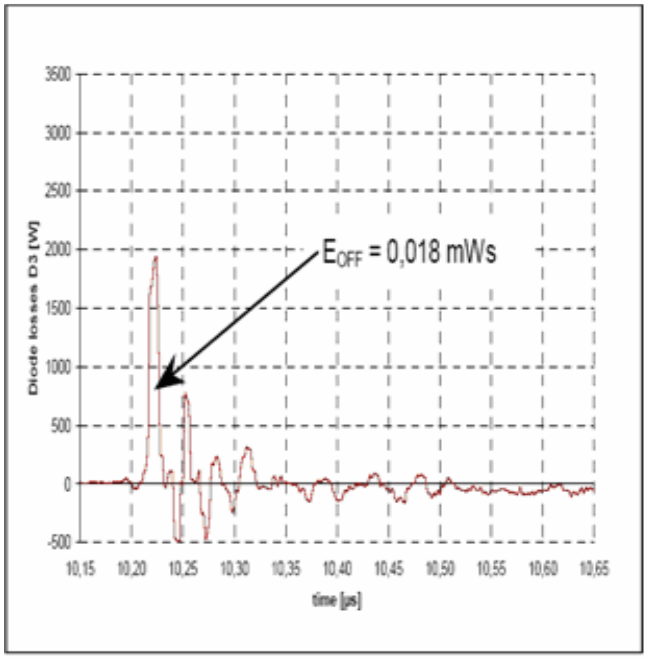

Fig.13: Switching off D3 with Sic Schottky diode